Observation of Critical Modes in Quasiperiodic Systems

Jean-Pierre Desideri, Louis Macon,[a] and Didier Sornette
Laboratoire de Physique de la Matière Condensée, Faculté des Sciences, Parc Valrose, 06034 Nice CEDEX, France
(Received 22 February 1989)

We present experimental results and their interpretation on the propagation of surface acoustic waves on a quasiperiodically corrugated solid. The surface is made of a thousand grooves engraved according to a Fibonacci sequence. For the first time, we observe the spatial structure of the critical proper modes obtained from an optical diffraction experiment. These special modes are characteristic of quasiperiodic systems and exhibit remarkable scaling features.

PACS numbers: 68.35.Gy, 03.40.Kf, 71.55.Jv

It is usually accepted that wave propagation in disordered structures leads to the phenomenon of Anderson localization[1] at any nonvanishing disorder for space dimensions $d=1$ and 2 and at sufficiently high disorder for $d=3$. The localization regime is a nonperturbative effect involving coherent interferences between all the wavelets partially reflected by the quenched disordered set of scatterers, for which only partial scenarios exist. According to the present wisdom, wave propagation in random media is characterized by the existence of a remarkable localization transition separating an "extended regime" at small disorder and a "localized regime" at large disorder, only at space dimension $d>2$. At lower dimensions, any nonvanishing disorder leads to the second regime. The existence of a transition between two regimes is always exciting because one can hope that understanding the crucial features which trigger the transition will reveal the physics of the different regimes.

In this respect, wave propagation in one-dimensional ($d=1$) quasiperiodic systems is very interesting since it has been discovered[2] that there exists a transition between an extended and a localized regime similarly to what occurs in $d=3$ disordered systems.[1] $d=1$ quasiperiodic systems are thus natural intermediate cases between periodicity and randomness. Another motivation for studying these systems follows from the recent experimental discovery of the quasicrystal phase in metallic alloys.[3] From a different point of view, since we have studied this problem in the context of surface acoustic waves (SAW's), the understanding of the interaction of elastic surface acoustic waves with complex surface topography[4,5] is of major importance to underwater acoustics, seismology, surface-acoustic-wave devices, nondestructive testing, and ultrasonic applications in medicine.

In this Letter, we report experimental measurements on the spectrum and the proper modes of a Rayleigh surface acoustic wave propagating on the quasiperiodically corrugated surface of a piezoelectric lithium niobate (YZ-$LiNbO_3$) substrate with a thousand grooves engraved according to a Fibonacci sequence. It is shown that this system is in the critical regime of the localization transition predicted to occur in certain quasiperiodic systems. With our choice of studying surface waves, an optical diffraction experiment using the Raman-Nath effect[6] allows us to probe for the first time the spatial structure of the proper modes with a remarkable precision, and to obtain information which is otherwise very difficult to extract experimentally. We verify that these modes exhibit remarkable scaling laws corresponding to a product of sinusoids with periods related to the different quasiperiods of the system.[7] The observed large-scale structures constitute the clearest signature of the criticality of these proper modes.

We have studied a lattice of $N=10^3$ identical grooves engraved, using well-known microlithographic techniques,[4] on the surface of a piezoelectric substrate of total length $L=15984$ μm. The average distance a between the grooves is thus $a=L/N=15.984\approx 16$ μm. Each groove has a width $w=5$ μm, a depth $h=0.3$ μm, and a well-characterized inverse plateau profile. The lateral scale of each groove (the so-called opening) is $E=2150$ μm. The groove centers are positioned on the sites of the Fibonacci sequence built recursively from the successive concatenation of lower-order patterns,[8]

$$S_{j+1}=\{S_{j-1},S_j\}\,. \tag{1}$$

One has $S_0=\{s\}$, $S_1=\{c\}$, $S_2=\{sc\}$, $S_3=\{csc\}$, $S_4=\{sccsc\}$, and so forth. $s=11.6\pm 0.1$ μm and $c=18.7\pm 0.1$ μm are the two elementary tiles of our one-dimensional quasicrystal. We have $s/c=0.620\pm 0.005$, near the inverse golden mean $t=(\sqrt{5}-1)/2=0.6180$. The ± 0.05-μm precision of the position of the grooves corresponds to the limitation of the electronic etching technique.

Our typical surface-acoustic-wave setup is composed of electromechanical transducers, laid down onto the surface of the YZ-$LiNbO_3$ crystal, which surround the array of etched grooves. The transducers are periodic structures of alternate interdigital electrodes connected to two buses, which are themselves connected to the terminals of either an electric generator or an analyzer. They perform the launching and detection of the surface acoustic waves both in reflection and transmission. The Rayleigh wave has well-known characteristics.[4] It is a mixture of longitudinal- and transverse-acoustic modes. It propagates along the solid-air plane boundary and is

evanescent away from the solid boundary with a typical excursion of the order of the wavelength ($\lambda \approx 20$ μm at typical frequencies around 170 MHz). Its phase velocity $c_R \approx 3490\ \mathrm{m\,s^{-1}}$ is slightly less than the transverse wave c_t and its dispersion is linear in the absence of surface corrugation. In the presence of a single groove, the SAW is partially reflected with a reflection amplitude coefficient given by $\mu \approx 0.6(h/\lambda)\sin(2\pi w/\lambda) \approx 10^{-2}$ for our frequency range. Furthermore, a fraction $p \sim 20\mu^2$ of the SAW energy is detrapped and converted into longitudinal and shear bulk acoustic waves.[4]

We first briefly present some of our most salient results and then discuss their significance. Figure 1 gives the dependence of the SAW reflection coefficient R as a function of frequency f in the range 153–193 MHz. The large-scale bell-like shape corresponds to the transfer function of the measuring transducers. The information relevant to the study of the $d=1$ quasicrystal is the peaks which decorate this structure. We observe the existence of particular frequencies f for which the reflection coefficient is significantly increased. This can be interpreted as the largest stop bands of the system. We have verified that the pattern of peaks obtained under reflection was recovered exactly under transmission.[9]

Figure 2 shows the spatial structure of the SAW at particular frequencies in the neighborhood of one of the gaps (shown by the arrow $at/\lambda = 8/17$ in Fig. 1). We note first that the intensity modulations have spatial periods $\Lambda \approx 10^2$–10^4 μm much larger than the period $\lambda/2 \approx 10$ μm of the standing waves that would occur in a cavity of size equal to the system length in the absence of the quasicrystalline lattice of grooves, for the short wavelengths used in our experiments. These modulations are thus interesting signatures of the SAW propagation on the quasiperiodic lattice. Figure 2 is obtained under a "zero-flux" condition, i.e., by superimposing two SAW's of approximately the same frequency, amplitude, and phase but opposite direction launched from the two transducers on both sides of the system. We have verified[9] that this SAW spatial structure has the same topology (same number of oscillations), apart from a difference in amplitude, as the one obtained when the SAW is launched from only one side of the system. This feature has been verified on many other examples at different frequencies. In Fig. 2, it can be noted that several different spatial periods are superimposed and build the complex spatial modulation of the wave. Note also the sensitivity of the largest spatial modulation with respect to SAW frequency: A frequency shift of 0.1 MHz (less than 10^{-3} in relative value) yields a transition from four undulations to three and from three to two undulations.

In order to rationalize these observations, we need a theory describing the SAW propagation over an array of grooves. For symmetric scatterers and from local energy flux conservation, we previously derived[10] a general transfer matrix connecting the SAW amplitude before and after a groove. Consider a wave amplitude at point x of the general form

$$Y_n(x) = Y_n^+ e^{ik(x-x_n)} + Y_n^- e^{-k(x-x_n)}$$

before the scatterer located at $x = x_n$ and

$$Y_{n+1}(x) = Y_{n+1}^+ e^{ik(x-x_n)} + Y_{n+1}^- e^{-ik(x-x_n)}$$

after the scatterer. Then, a transfer matrix M connects $\{Y_{n+1}^+, Y_{n+1}^-\}$ to $\{Y_n^+, Y_n^-\}$. Neglecting wave attenua-

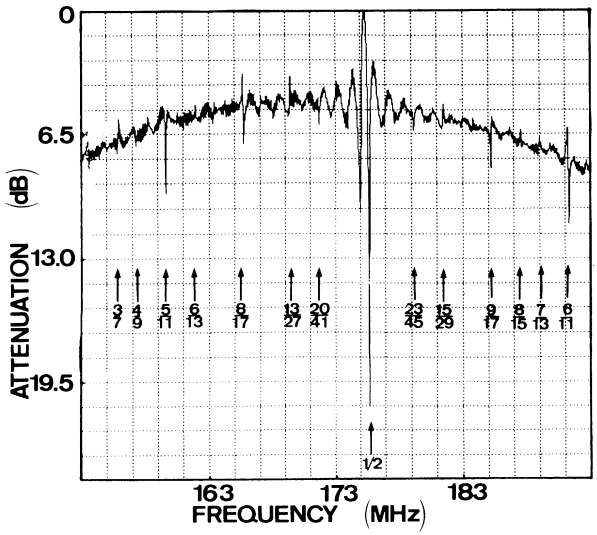

FIG. 1. Dependence of the SAW reflection modulus as a function of frequency. Each peak probes the existence of a stop band (see Ref. 9 for more details about the peak pattern).

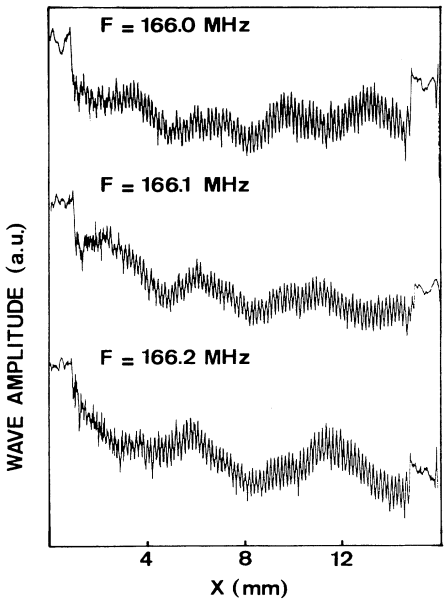

FIG. 2. SAW intensity as a function of position of the laser spot along the sample for three close frequencies in the neighborhood of one stop band shown in Fig. 1 ($at/\lambda = 8/17$).

tion, M becomes symplectic and depends on two parameters μ_n and ϕ_n, where μ_n is the groove amplitude reflection coefficient which is constant in our case ($\mu_n=\mu$) and $\phi_n=k(x_{n+1}-x_n)$, with $k=2\pi/\lambda$, represents the phase factor for the propagation from the $(n-1)$th to the nth groove. The transfer-matrix formalism can be mapped onto a discrete off-diagonal Schrödinger tight-binding equation[8] in terms of the value $Y_n=Y_n^+ + Y_n^-$ of the SAW amplitude just before the nth groove:

$$t_{n+1}Y_{n+1}+t_{n-1}Y_{n-1}-E_nY_n=0\,, \tag{2}$$

with $t_{n+1}=\sin\phi_{n-1}$, $t_{n-1}=\sin\phi_n$, and

$$E_n=\sin(\phi_{n-1}+\phi_n)-2\mu\sin\phi_{n-1}\sin\phi_n\,.$$

Note that the quasiperiodic modulation of the grooves enters only via the phases ϕ_n. In contrast to the Aubry model[2] where the scatterers are equidistant but have *scattering cross sections* quasiperiodically modulated [$t_{n-1}=t_{n+1}=t$ is constant and $E=V\cos(2\pi nt)$], Eq. (2) corresponds to identical scatterers, with *positions* given by the inflation rule (1). The ϕ_n thus takes only two values $\phi_c=kc$ and $\phi_s=ks$ which occur according to the formula

$$\phi_n=(2\pi/\lambda)[c-(c-s)\mathrm{int}\{\mathrm{frac}(n(t-1))-t\}]\,, \tag{3}$$

where int(x) means the integer part of x, and frac(x) mean the fractional part of x. In this case, the spectrum is predicted to be a Cantor set with zero Lebesgue measure. This system is also argued to correspond to the critical condition $V=2t$ (Ref. 11) of the Aubry model.[12] The proper modes are neither extended nor localized and exhibit a characteristic scaling.[7] The precise features of the spectrum and the proper modes can be obtained from a mapping theory written in terms of the trace of the transfer matrix which obeys a simple nonlinear map.[12] In general, this map can only be studied numerically. As a complementary picture, we present a heuristic model for the SAW propagation, which relies on the tight-binding Schrödinger discrete equation (2) and which allows us to interpret quantitatively our experimental results.[9]

Our approach amounts to replacing the exact expression (3) for the ϕ_n by the following *Ansatz*:

$$\phi_n=2\pi\,\mathrm{frac}\{nat/\lambda\}\,. \tag{4}$$

Numerical justification of the *Ansatz* will be reported in Ref. 9. Equation (4) is very similar to Eq. (3) but for the fact that the wavelength λ now appears inside the function frac. Inserting expression (4) into (2) shows that the coefficients of Eq. (2) are now of the form $\sin[2\pi nat/\lambda+\varphi(\mu)]$ since a periodic function of ϕ_n makes it possible to eliminate the function frac. For wavelengths such that at/λ is a rational number p/q, the response of the system is thus similar to that of a periodic structure of period q. The smallest q will give the largest reflection coefficient since this will correspond to the largest number of periods per unit length in the effective periodic lattice. This is indeed what one can observe in Fig. 1: A series of peaks in the neighborhood of the central frequency $f\approx 175$ MHz can be indexed by a single integer n such that the variable at/λ is of the form

$$at/\lambda=n/(2n\pm 1),\quad n=1,2,\ldots,\infty\,. \tag{5}$$

The series (5) corresponds to very favorable cases (q small) and gives the strongest reflection coefficients. Consider, for instance, the case $at/\lambda=0.5$. The measured width of this stop band, obtained by magnification of Fig. 1, is $\Delta f=0.7\pm 0.1$ MHz yielding $\Delta f/f\approx(4\pm 0.5)\times 10^{-3}$. The theoretical value corresponds to the two wavelengths such that $(1+\mu^2/2)\cos 2\pi at/\lambda=1$ which gives $\Delta f/f_{\mathrm{theor}}\approx 5.7\times 10^{-3}$ in rather good agreement with the experimental value. Good quantitative agreement also carries over to the other peaks.

Let us now explain the striking structure of the proper modes presented in Fig. 2. From our *Ansatz* (4) and the implicit existence of an equivalent periodic system, one expects that the modes should have a structure corresponding to that of the Bloch modes in these effective periodic systems. In the case of Fig. 2, at/λ is in the neighborhood of 8/17 with frequency around $f\approx 166$ MHz. Consider more precisely the mode at $f=166.0$ MHz. With $c_R\approx 3490$ m s^{-1},[4,9] this yields $at/\lambda=237/504$.[13] The successive diophantine approximations of this rational number are 1/2, 7/15, 8/17, and 237/504 since its continued-fraction expansion is

$$\begin{aligned}237/504&=(r_1+(r_2+(r_3+r_4^{-1})^{-1})^{-1})^{-1}\\&=(2+(7+(1+9^{-1})^{-1})^{-1})^{-1}\,.\end{aligned}$$

Because of the fact that we observe experimentally the envelope of the wave amplitude, this implies that one should observe the spatial periods a, $(7-8)a$, and $252a$ corresponding, respectively, to the first approximation $r_1=2$, to the second (and third) approximation $r_2=7$ ($r_3=1$),[14] and to the fourth approximation $r_4=9$. These different periods 1, 7–8, and 252 correspond to a total number of oscillations over the system length $L/a=10^3$ equal, respectively, to 1000/1, 1000/8=125, and 1000/252$\approx$4. These predictions are well observed in Fig. 2 for the largest periods 7–8 and 252. Because of the finite spatial resolution of the optical probing method, we cannot see the shortest period a. Note that these observations are similar to the proposal by Thouless and Niu[7] concerning the large-scale spatial structure of a critical proper mode.

The same analysis can be repeated for all modes. By carefully spanning the SAW frequency range, we have observed as many as three different sinusoidal modulations with largely different wavelengths which superimpose and determine the spatial structure of the mode. Note that the appearance of long-wavelength modulations as occurs in Fig. 2 corresponds to a very rapid con-

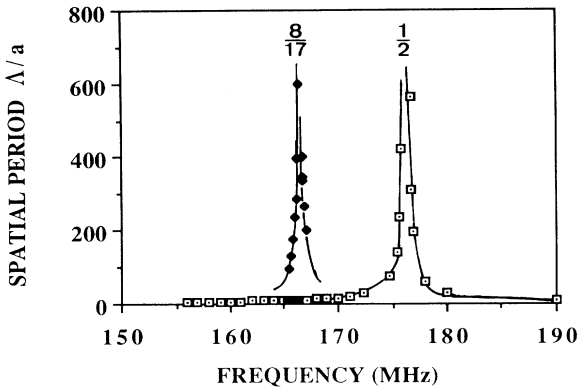

FIG. 3. Spatial period Λ of the observable proper modes for frequencies in the neighborhood of two stop bands shown in Fig. 1: $at/\lambda = 1/2$ (right peak) and $at/\lambda = 8/17$ (left peak).

vergence of the successive diophantine approximation p_n/q_n of at/λ. The larger q_n is, the smaller will be the frequency range over which the diophantine approximation holds at the order n. This is illustrated in Fig. 3: The bandwidth and the frequency interval over which the tail of the peak survives are larger for $at/\lambda = 1/2$ than for 8/17. This also explains the transitions observed in Fig. 2 where only the largest period is sensitive to a small frequency shift.

As f approaches a stop-band edge (5), the largest spatial modulation Λ diverges, as seen in Fig. 3 for the two cases $at/\lambda = 1/2$ and 8/17, according to a measured power law[9] $\Lambda \sim |f - f_{1/2}|^{-\nu}$ with $\nu = 0.50 \pm 0.05$. Consider the Bloch expression for the mode amplitude $Y_n(x) = u_n(x)e^{-iKx}$, with $u_n(x)$ of period qa and K given by $s = e^{\pm iKqa}$. The quantity s verifies the secular equation $s^2 - \{\text{trace}(M)\}s + 1 = 0$, M being the corresponding transfer matrix over a single cell. In the neighborhood of band edges, one has generically $\text{trace}(M) \to 2$, which implies that s is close to one and K is close to zero. The sinusoidal modulation e^{-iKx} develops therefore a very long spatial period

$$\Lambda = qa(Kqa)^{-1} \approx qa(1-s)^{-\nu} = qa\,|2 - \text{trace}(M)|^{-\nu},$$

with $\nu = \frac{1}{2}$ in agreement with our fit. This power law can be verified for all frequencies such that at/λ fulfills Eq. (5).

In summary, we have given, for the first time, an experimental characterization of the critical proper modes in $d = 1$ quasiperiodic systems. Their spatial structure can be simply interpreted in terms of successive diophantine approximations of the reduced variable at/λ, where a is the average lattice period, λ is the surface acoustic wavelength, and t is the inverse golden mean. A much extended version of this work is presented in Ref. 9 where the time impulse response is also discussed. The theory is developed and provides a means to escape from the approximation (4) used instead of (3). By a full treatment of the complete problem (3), the experimental results are explained in terms of the asymptotic approximation of the quasicrystal by periodic systems of increasing periods.

We are grateful to J. F. Gelly and C. Maerfeld for their kind welcome at Thomson-Sintra at Sophia-Antipolis where the experiments have been carried out. We acknowledge financial support from Direction des Recherches, Etudes et Techniques under Contract No. 86/177 for the research program "Propagation acoustique en milieux aléatoires." Laboratoire de Physique de la Matière Condensée is CNRS URA 190.

[a]Now at SPECTEC S.A., 14 Av. St. Augustin, 06300 Nice, France.

[1]See, for example, B. Souillard, in *Chance and Matter,* Proceedings of the Les Houches Summer School, Session XLVI, edited by J. Souletie, J. Vannimenus, and R. Stora (North-Holland, Amsterdam, 1987), and references therein; D. Sornette, Acustica **67**, 199 (1989); **67**, 251 (1989); **68**, 15 (1989).

[2]S. Aubry, Solid State Sci. **8**, 264 (1978); G. André and S. Aubry, Ann. Israel Phys. Soc. **3**, 133 (1989).

[3]D. Shechtman, I. Blech, D. Gratias, and J. W. Cahn, Phys. Rev. Lett. **53**, 1951 (1984).

[4]*Rayleigh-Wave Theory and Application,* edited by E. A. Ash and E. G. S. Paige, Springer Series on Wave Phenomena Vol. 2 (Springer-Verlag, Berlin, 1985).

[5]J. R. Chamuel and G. H. Brooke, J. Acoust. Soc. Am. **84**, 1363 (1988).

[6]J. P. Monchalin, IEEE Trans. Ultrason. Ferr. Freq. Control **33**, 485 (1986).

[7]D. J. Thouless and Q. Niu, J. Phys. A **16**, 1911 (1983).

[8]See, for example, J. B. Sokoloff, Phys. Rep. **126**, 189 (1985).

[9]L. Macon, J. P. Desideri, and D. Sornette, "Localization of surface acoustic waves in a quasi-crystal" (to be published).

[10]D. Sornett, L. Macon, and J. Coste, J. Phys. (Paris) **49**, 1683 (1988).

[11]The Aubry model is characterized by two regimes: For $V > 2t$, all eigenfunctions are localized and the spectrum is pure point, whereas for $V < 2t$, all eigenfunctions are extended and the spectrum is continuous.

[12]M. Kohmoto, L. P. Kadanoff, and C. Tang, Phys. Rev. Lett. **50**, 1870 (1983).

[13]Because of the finite size $L/a = 10^3$ of the system, there is no meaning in giving a rational approximation p/q of at/λ with q much larger than $L/2a$ since this would correspond to periods larger than the system size.

[14]The periods 7 and 8 cannot be distinguished and give a long-wavelength beating of size L.